



Cite this: *Chem. Commun.*, 2015, 51, 14247

Received 16th July 2015,
Accepted 5th August 2015

DOI: 10.1039/c5cc05909g

www.rsc.org/chemcomm

Mixed monolayer protected gold nanoparticles were prepared featuring functional groups on their surfaces that can engage in interactions with peptides. DOSY NMR binding studies indicate that nanoparticles containing a combination of three orthogonal functional groups are more efficient in binding to dipeptides than mono or difunctionalised analogues.

The design of a synthetic receptor typically involves arranging suitable binding sites on a molecular scaffold that mediate the interaction with a structurally complementary substrate. While this strategy afforded numerous potent receptors in the past, it is usually associated with a considerable synthetic effort. A conceptually more straightforward approach involves the use of a core structure for receptor development that allows easy decoration with a wide range of different recognition units. In this context, nanoparticles, in particular gold nanoparticles (AuNPs), have recently emerged as a versatile platform for the development of polyfunctional receptors and chemosensors with applications in biology, medicine, or catalysis.¹

AuNPs are relatively easy to prepare with controllable size distributions thus allowing regulation of surface curvature and number of functional groups on the gold core. They are stable in solution once they are protected with appropriate ligands such as organic thiols. They can be made soluble in a wide range of solvents, including water, by varying the structures of the surface-bound ligands. The optical properties of AuNPs allow the facile development of sensing systems,² and substrate recognition (including the subsequent catalytic transformation of the substrate) can benefit from multivalent effects, or from cooperativity of different functional groups on the surface.³

Dipeptide recognition in water mediated by mixed monolayer protected gold nanoparticles†

Serap Yapar,^a Maria Oikonomou,^b Aldrik H. Velders^b and Stefan Kubik^{*a}

The size of AuNPs, which is typically in a similar range as that of small proteins or nucleic acids, renders AuNPs particularly useful for designing receptors that selectively attach to protein surfaces or DNA sequences.⁴ In addition, a number of AuNP-based receptors that bind to low molecular weight compounds have been described. Examples are Rotello's flavine receptor,⁵ Scrimin's AuNPs that catalytically cleave esters or phosphodiesterases,⁶ the receptors for nucleotide triphosphates developed by Prins,⁷ and Rastrelli's and Mancin's salicylaldehyde receptor.⁸ Yet AuNP-based receptors for small peptides such as dipeptides are rare‡ and we wondered whether they could be accessible by using known strategies for developing covalently constructed peptide receptors.⁹ In this context, we took inspiration from a classical receptor described by Hossain and Schneider.¹⁰ This compound contains a crown ether moiety and a quaternary ammonium ion along a rigid scaffold for binding to the N- and the C-terminal ends of an unprotected peptide, respectively. Both binding sites were carefully chosen such that they do not interact with each other so that intramolecular conformational collapse of the receptor or its intermolecular self-aggregation is avoided. An aromatic moiety was introduced as a third binding site to induce selectivity for peptides with aromatic side chains. The corresponding receptor was shown to interact with dipeptides and tripeptides in methanol and water and indeed exhibited improved affinity for peptides with aromatic side chains in some cases.

Based on this concept we devised analogous mixed monolayer protected AuNPs and investigated their interaction with dipeptides in water. Introduction of the functional groups required for peptide recognition was achieved by decoration of AuNPs with the α,ω -functionalised thiols **Q**, **C** and **P** containing as recognition elements a terminal trimethylalkyl ammonium group, an 18-crown-6 moiety, and a phenyl group, respectively (Fig. 1, for ligand syntheses, see ESI†).

AuNP synthesis was achieved by first preparing dioctylamine-protected nanoparticles and subsequently replacing the weakly bound amine ligands with the functionalised thiols. This strategy has the advantage of allowing a more straightforward control over the ratio of different ligands on the AuNPs surface than the

^a Technische Universität Kaiserslautern, Fachbereich Chemie - Organische Chemie, Erwin-Schrödinger-Straße, D-67663 Kaiserslautern, Germany.
E-mail: kubik@chemie.uni-kl.de

^b Laboratory of BioNanoTechnology, Wageningen University, Dreijenplein 6, 6703 HB Wageningen, The Netherlands

† Electronic supplementary information (ESI) available: Syntheses and characterisation of the ligands and the prepared AuNPs, experimental details of the DOSY NMR spectroscopic binding studies. See DOI: 10.1039/c5cc05909g



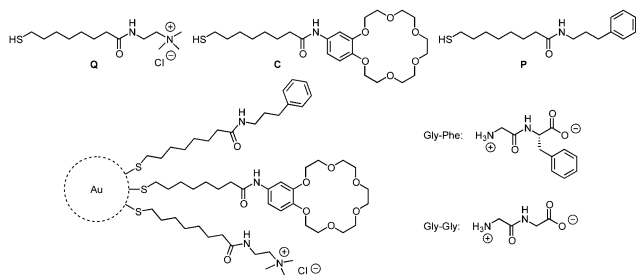


Fig. 1 Ligands **Q**, **C**, **P**, schematic representation of the AuNPs prepared thereof using **NP_{QPC}** as an example, and structures of the peptides used as substrates.

alternative strategy starting from thiol protected AuNPs and thiol exchange reactions.¹¹ After purification of the obtained AuNPs by microfiltration the ¹H NMR spectra exhibited broad signals of the ligands (see Fig. S8, ESI[†]) indicating successful ligand attachment to the gold surface and the absence of unbound species. Altogether four AuNPs were thus prepared, **NP_Q** containing only ammonium groups on the surface and AuNPs **NP_{QC}**, **NP_{QP}**, and **NP_{QPC}** containing, respectively, ligands **C**, **P**, or a mixture thereof in addition to **Q**. Nanoparticles without ammonium groups turned out to be insufficiently soluble to allow binding studies in water.

The prepared AuNPs were characterised by UV/vis spectroscopy, transmission electron microscopy (TEM), and DOSY NMR spectroscopy. In the UV/vis spectrum of an **NP_Q** solution in water a very weak absorption band at ca. 515 nm was observed (see Fig. S9, ESI[†]), indicating that the average diameter of these AuNPs is around 2 nm.¹² The TEM images of the four AuNPs revealed mostly small particles with a relatively narrow size distribution and only few larger particles (see Fig. S10–S13, ESI[†]). The average diameters d_{TEM} of the gold cores estimated from the TEM images are summarised in Table 1. This table also contains the hydrodynamic diameters of the prepared AuNPs calculated by using the Stokes–Einstein equation from the diffusion coefficients measured by DOSY NMR.¹³ Comparison of d_{DOSY} with the corresponding d_{TEM} values indicates that the surface layers of the AuNPs have thicknesses of ca. 1.6 nm.

The ratio of the different ligands on these AuNPs could not be estimated directly from the ¹H NMR spectra because of pronounced signal broadening. Therefore, the nanoparticles were decomposed and the ligands released by addition of iodine to a nanoparticle solution in methanol- d_4 .¹⁴ The ¹H NMR spectra of

Table 1 Averaged diameters of mixed monolayer protected AuNPs **NP_Q**, **NP_{QC}**, **NP_{QP}**, and **NP_{QPC}**

AuNP	$d_{\text{TEM}}^a/\text{nm}$	$D^b/\text{m}^2 \text{ s}^{-1}$	$d_{\text{DOSY}}^c/\text{nm}$
NP_Q	1.9	8.1×10^{-11}	5.0
NP_{QC}	2.5	7.2×10^{-11}	5.6
NP_{QP}	2.6	7.4×10^{-11}	5.5
NP_{QPC}	1.9	8.0×10^{-11}	5.0

^a Average diameters determined by transmission electron microscopy.

^b Diffusion coefficients determined by DOSY NMR spectroscopy in D₂O (99.96%) at 300 K. ^c Hydrodynamic diameters calculated from D by using the Stokes–Einstein equation.

Table 2 Relative amounts of ligands **Q**, **C**, and **P** on the surfaces of AuNPs **NP_Q**, **NP_{QC}**, **NP_{QP}**, and **NP_{QPC}**^a

AuNP	Q /%	C /%	P /%	Average composition
NP_Q	100			Au ₂₁₁ Q ₄₉
NP_{QC}	53	47		Au ₄₈₁ Q _{52.5} C _{46.5}
NP_{QP}	47		53	Au ₅₄₁ Q _{54.0} P _{61.0}
NP_{QPC}	48	25	27	Au ₂₁₁ Q _{24.5} C _{12.8} P _{13.7}

^a Determined ¹H NMR spectroscopically after iodine decomposition of the respective nanoparticle, with an estimated error of $\pm 5\%$.

the respective solutions exhibited sharp signals, which allowed calculation of the relative amount of each ligand in the mixture by integration of characteristic ligand signals. By performing these measurements in the presence of an internal standard with known concentration also allowed assessing the total amount of ligands on each nanoparticles as well as average nanoparticle composition (Table 2, for details, see ESI[†]). The obtained compositions are in good agreement with compositions calculated for such AuNPs by using the theoretical model proposed by Leff *et al.*¹⁵

Reproducibility of the results summarised in Table 2 for different AuNP batches turned out to be good indicating that the chosen synthetic strategy allows a reliable control over surface composition. Table 2 shows that all AuNPs contain at least ca. 50% of ligand **Q** to ensure water solubility. The other half is made up of either the same type of ligand in the case of **NP_Q**, another ligand type in the case of **NP_{QC}** and **NP_{QP}**, or an approximate 1 : 1 mixture of ligands **C** and **P** in the case of **NP_{QPC}**. In light of their overall average compositions, these nanoparticles likely feature surface arrangements with functional groups of different ligands located in close proximity, potentially allowing cooperative action in substrate binding.

To evaluate whether ¹H NMR spectroscopy is a suitable method to quantify binding of peptides to the prepared AuNPs, increasing amounts of **NP_Q** were added to a solution of the dipeptide Gly–Gly in D₂O. Small but clearly visible downfield shifts of peptide signals were observed when increasing the AuNP concentration, indicating an interaction between the dipeptide and the nanoparticles (see Fig. S16, ESI[†]). The extent of these shifts combined with pronounced overlaps with AuNP signals did not allow using this method for the quantification of binding strength, however. In the case of Gly–Phe, the position and multiplicity of some peptide signals further complicated ¹H NMR spectroscopic binding studies. We therefore turned to DOSY NMR spectroscopy to gain insight into the correlation of surface composition and peptide affinity.

The evaluation of binding equilibria that are fast on the NMR timescale by DOSY NMR spectroscopy is based on the reduction of the diffusion coefficient of a small molecule once it binds to a larger receptor. The resulting diffusion coefficient D_{obs} represents a weighted average of the coefficients of the free and the bound states.¹³ The fraction χ of bound substrate in an equilibrium can thus be calculated from D_{obs} , the diffusion coefficients of the free substrate D_{free} , and that of the complex D_{bound} . The latter is usually assumed to equal the diffusion complex of free receptor. This method has, for example, been applied to evaluate binding of 2,3-bisphosphoglycerate to haemoglobin,¹⁶



Table 3 Fractions χ of bound dipeptides to the functionalised nanoparticles^a

AuNP	χ (Gly-Phe)/%	χ (Gly-Gly)/%
NP_Q	38	32
NP_{QC}	31	23
NP_{QP}	21	19
NP_{QPC}	78	48

^a Determined by DOSY NMR spectroscopy in D₂O (99.96%) at 300 K and total ligand concentrations of 1.9 ± 0.1 mM and peptide concentrations of 0.072 mM.

alcohols to cyclodextrins,¹⁷ neurotransmitters to micelles,¹⁸ and also carboxylates to oppositely charged monolayer-protected gold nanoparticles.^{8b} The advantage is that comparing the extent to which a specific substrate binds to different receptors under identical conditions directly provides information about the relative substrate affinities of the respective receptors. To ensure comparability of the results, all measurements were performed at approximately the same overall concentration of the surface-bound ligands of the different AuNPs. The results of these binding studies, which involved the use of dipeptides Gly-Gly and Gly-Phe as substrates and D₂O as solvent, are summarised in Table 3.

Table 3 shows that the DOSY NMR measurements provide clear evidence for the interaction between the peptides and the AuNPs. Moreover, the determined fractions of bound peptides χ depend on the functional groups present on the particles. AuNP **NP_Q**, containing only quaternary ammonium ions binds to Gly-Gly and Gly-Phe with similar affinity, presumably by electrostatic interactions between the ammonium groups on the AuNP surfaces and the peptide carboxylate groups. The additional presence of the crown ether in **NP_{QC}** or the aromatic groups in **NP_{QP}** has a small and not necessarily beneficial effect on the overall affinity although it must be considered that these AuNPs only contain half the number of the quaternary ammonium groups in comparison to **NP_Q**. Thus, in contrast to Schneider's low molecular weight receptor a cooperativity of the ammonium and the crown ether groups in binding to the terminal ends of short peptides could not be observed for **NP_{QC}**, which may be due to the fact that the orthogonal binding sites are arranged in relatively close proximity on the AuNP surface and not separated by a rigid linker as in Schneider's receptor.⁹ Nanoparticle **NP_{QPC}**, however, exhibits a higher affinity than the other AuNPs, maybe because the presence of additional aromatic units is required to "dilute" the binding sites and to induce arrangements with larger distances, thus allowing the quaternary ammonium ions and crown ether moieties to cooperatively bind to the peptides. This effect is substantially more pronounced for Gly-Phe binding, indicating that aromatic interactions are likely to contribute to complex stability.

To evaluate peptide binding quantitatively, DOSY NMR titrations were performed with **NP_Q** and **NP_{QPC}** during which the Gly-Phe concentrations were progressively increased while keeping those of the nanoparticles constant. The resulting χ values were plotted against peptide concentration and the obtained curves were fitted to Langmuir isotherms (Fig. 2, for details, see ESI†).¹⁹ The adsorption equilibrium constants K thus obtained amount to 4770 ± 1180 M⁻¹ for **NP_Q** and 8260 ± 1480 M⁻¹ for **NP_{QPC}**

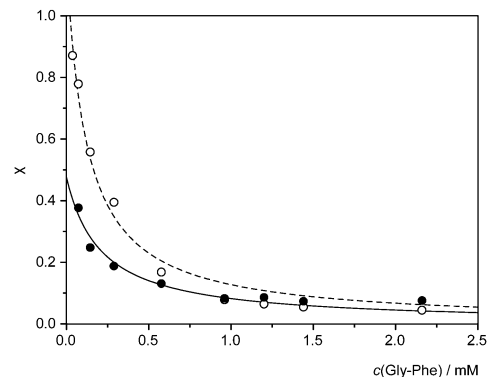


Fig. 2 Dependence of the DOSY NMR spectroscopically determined fraction of bound Gly-Phe to **NP_Q** (filled circles) and **NP_{QPC}** (open circles) on peptide concentration and fitting of the data to Langmuir isotherms. The points represent the experimental data and the lines the fitted curves.

(for other synthetic batches of these AuNPs equilibrium constants of 3880 ± 860 M⁻¹ and 6090 ± 1380 M⁻¹ were observed, respectively), clearly confirming the increase of peptide affinity upon combining the three ligands on the nanoparticle surface. The Langmuir treatment also yielded the maximum concentration of bound peptides as a second fitted parameter, which showed that **NP_Q** and **NP_{QPC}** bind, respectively, 2.6 and 3.6 peptide molecules on average.

In conclusion, this work shows that combining different functional groups on the surface of AuNPs affords receptors for low molecular weight compounds, in this case for peptides. The individual functional groups on these AuNPs contribute to substrate recognition by presenting specific binding sites and/or surface arrangements suitable for substrate binding. The attractiveness of the presented approach lies in the ease with which the receptors can be prepared once a library of functional thiols is available and its enormous flexibility. We are currently investigating whether the lack over controlling surface structure associated with the current synthetic strategy can be circumvented by performing AuNP synthesis under the influence of template effects of the substrates.²⁰ The results of these efforts will be reported in due course.

Funding of this work through the Marie Curie Initial Training Network on Dynamic Molecular Nanostructures (DYNAMOL) is gratefully acknowledged. We also thank Jan Bart ten Hove at Wageningen University for help with the TEM measurements.

Notes and references

‡ The cationic nanoparticles described by Scrimin⁶ and Prins⁷ contain negatively charged peptides as catalytically active sites or sensing units.

- R. Shenhar and V. M. Rotello, *Acc. Chem. Res.*, 2003, **36**, 549–561; R. A. Sperling, P. R. Gil, F. Zhang, M. Zanella and W. J. Parak, *Chem. Soc. Rev.*, 2008, **37**, 1896–1908; R. Wilson, *Chem. Soc. Rev.*, 2008, **37**, 2028–2045; A. Corma and H. Garcia, *Chem. Soc. Rev.*, 2008, **37**, 2096–2126; D. A. Giljohann, D. S. Seferos, W. L. Daniel, M. D. Massich, P. C. Patel and C. A. Mirkin, *Angew. Chem., Int. Ed.*, 2010, **49**, 3280–3294; Y.-C. Yeh, B. Creran and V. M. Rotello, *Nanoscale*, 2012, **4**, 1871–1880; L. Dykman and N. Khlebtsov, *Chem. Soc. Rev.*, 2012, **41**, 2256–2282.
- N. L. Rosi and C. A. Mirkin, *Chem. Rev.*, 2005, **105**, 1547–1562; K. Saha, S. S. Agasti, C. Kim, X. Li and V. M. Rotello, *Chem. Rev.*, 2012, **112**, 2739–2779.



- 3 C. Fasting, C. A. Schalley, M. Weber, O. Seitz, S. Hecht, B. Kokschi, J. Dervedde, C. Graf, E.-W. Knapp and R. Haag, *Angew. Chem., Int. Ed.*, 2012, **51**, 10472–10498; G. Pieters and L. J. Prins, *New J. Chem.*, 2012, **36**, 1931–1939.
- 4 A. Verma and V. M. Rotello, *Chem. Commun.*, 2005, 303–312.
- 5 A. K. Boal and V. M. Rotello, *J. Am. Chem. Soc.*, 2000, **122**, 734–735; A. Bayir, B. J. Jordan, A. Verma, M. A. Pollier, G. Cooke and V. M. Rotello, *Chem. Commun.*, 2006, 4033–4035.
- 6 F. Manea, F. B. Houillon, L. Pasquato and P. Scrimin, *Angew. Chem., Int. Ed.*, 2004, **43**, 6165–6169; R. Bonomi, F. Selvestrel, V. Lombardo, C. Sissi, S. Polizzi, F. Mancin, U. Tonellato and P. Scrimin, *J. Am. Chem. Soc.*, 2008, **130**, 15744–15745; G. Zaupa, C. Mora, R. Bonomi, L. J. Prins and P. Scrimin, *Chem. – Eur. J.*, 2011, **17**, 4879–4889; D. Zaramella, P. Scrimin and L. J. Prins, *J. Am. Chem. Soc.*, 2012, **134**, 8396–8399; M. Diez-Castellnou, F. Mancin and P. Scrimin, *J. Am. Chem. Soc.*, 2014, **136**, 1158–1161.
- 7 G. Pieters, A. Cazzolaro, R. Bonomi and L. J. Prins, *Chem. Commun.*, 2012, **48**, 1916–1918; G. Pieters, C. Pezzato and L. J. Prins, *Langmuir*, 2013, **29**, 7180–7185; C. Pezzato, B. Lee, K. Severin and L. J. Prins, *Chem. Commun.*, 2013, **49**, 469–471; S. Maiti, C. Pezzato, S. G. Martin and L. J. Prins, *J. Am. Chem. Soc.*, 2014, **136**, 11288–11291; C. Pezzato, D. Zaramella, M. Martinelli, G. Pieters, M. A. Pagano and L. J. Prins, *Org. Biomol. Chem.*, 2015, **13**, 1198–1203.
- 8 (a) B. Perrone, S. Springhetti, F. Ramadori, F. Rastrelli and F. Mancin, *J. Am. Chem. Soc.*, 2013, **135**, 11768–11771; (b) M.-V. Salvia, F. Ramadori, S. Springhetti, M. Diez-Castellnou, B. Perrone, F. Rastrelli and F. Mancin, *J. Am. Chem. Soc.*, 2015, **137**, 886–892.
- 9 H.-J. Schneider, *Angew. Chem., Int. Ed.*, 1993, **32**, 848–850; M. W. Pecuh and A. D. Hamilton, *Chem. Rev.*, 2000, **100**, 2479–2494.
- 10 M. A. Hossain and H.-J. Schneider, *J. Am. Chem. Soc.*, 1998, **120**, 11208–11209.
- 11 N. R. Jana and X. Peng, *J. Am. Chem. Soc.*, 2003, **125**, 14280–14281; F. Manea, C. Bindoli, S. Polizzi, L. Lay and P. Scrimin, *Langmuir*, 2008, **24**, 4120–4124.
- 12 G. A. Rance, D. H. Marsh and A. N. Khlobystov, *Chem. Phys. Lett.*, 2008, **460**, 230–236.
- 13 Y. Cohen, L. Avram and L. Frish, *Angew. Chem., Int. Ed.*, 2005, **44**, 520–554.
- 14 A. C. Templeton, M. J. Hostetler, C. T. Kraft and R. W. Murray, *J. Am. Chem. Soc.*, 1998, **120**, 1906–1911.
- 15 D. V. Leff, P. C. Ohara, J. R. Heath and W. M. Gelbart, *J. Phys. Chem.*, 1995, **99**, 7036–7041.
- 16 A. J. Lennon, N. R. Scott, B. E. Chapman and P. W. Kuchel, *Biophys. J.*, 1994, **67**, 2096–2109.
- 17 R. Rymdén, J. Carlfors and P. Stilbs, *J. Inclusion Phenom.*, 1983, **1**, 159–167.
- 18 G. Gattuso, A. Notti, S. Pappalardo, M. F. Parisi, I. Pisagatti and S. Patanè, *New J. Chem.*, 2014, **38**, 5983–5990.
- 19 R. D. Ross and R. K. Roeder, *J. Biomed. Mater. Res., Part A*, 2011, **99**, 58–66; S. H. Brewer, W. R. Glomm, M. C. Johnson, M. K. Knag and S. Franzen, *Langmuir*, 2005, **21**, 9303–9307.
- 20 F. della Sala and E. R. Kay, *Angew. Chem., Int. Ed.*, 2015, **54**, 4187–4191; P. Nowak, V. Saggiomo, F. Salehian, M. Colomb-Delsuc, Y. Han and S. Otto, *Angew. Chem., Int. Ed.*, 2015, **54**, 4192–4197.

